Gamma Ray Bursts and Afterglow

Re'em Sari

Theoretical Astrophysics 130-33, California institute of Technology, Pasadena CA 91125

Abstract. The origin of GRBs have been a mystery for almost 30 years. Their sources emit a huge amount of energy on short time scales and the process involves extreme relativistic motion with bulk Lorentz factor of at least a few hundred. In the last two years, "afterglow", emission in X-ray, optical, IR, and radio was detected. The afterglow can be measured up to months and even years after the few seconds GRB. We review the theory for the γ-rays emission and the afterglow and show that it is strongly supported by observations. A recent detection of optical emission simultaneous with the GRB, well agrees with theoretical predictions and further constrains the free parameters of the models. We discuss the evidence that some of the bursts are jets, and discuss the prospects of polarization measurements.

I THE GENERIC PICTURE

The phenomena of GRBs was discovered almost thirty years ago, by the Vela defense satellites [1]. Today, the biggest catalog of GRBs [2] is due to the instrument BATSE on board of the Compton Gamma-ray Observatory. BATSE observes about one burst per day and more than two thousands bursts have been observed by now. The spectrum of GRBs is well described by a broken powerlaw, and usually peaks between 100keV-400keV [3]. In strong bursts, high energy powerlaw tails extending up to 200 MeV were seen and the most extreme case had a few GeV photons detected. On the average the high energy tail is characterized by $\nu F_\nu \sim \nu^{-0.25}$. The duration of the GRBs varies significantly, mainly between a few milliseconds to a few hundred seconds. One of the striking properties of GRBs is their erratic temporal structure. While only a few burst are smooth, most of them vary over a time scale δt which is much shorter than the burst's duration t. In many bursts the ratio $N \equiv t/\delta t \geq 100$.

The cosmological distance to the bursts (now well established due to detection of redshifts), combined with the large fluence observed at earth implies that the energy released in the event is huge, with a record of 3×10^{54}erg (GRB 990123, see e.g. [4]). This huge energy, together with the short variability time scale, places the GRBs phenomena as the most extreme in the universe.

The extreme characteristics of GRBs lead to a paradox, so called the "compactness problem". If one assumes that an energy of 10^{52}erg made of photons,

CP510, *The Fifth Compton Symposium*, edited by M. L. McConnell and J. M. Ryan

distributed according to the GRBs spectrum, is released in a small volume of linear dimensions $R \leq c\delta t$ then the optical depth to pair creation is $\tau \sim 10^{15}$. If that was true, all the photons would have interacted to create pairs and thermalize. However, the observed spectrum of GRBs is highly non-thermal!

The only known solution to the "compactness problem" is relativistic motion. If the emission site is moving relativistically, with a Lorentz factor γ, toward the observer, then the optical depth is reduced, compared to the stationary estimate, due to two effects: First, the size of the source can be bigger by a factor of γ^2. This will still produce variability over a short time scale given by $\delta T = R/\gamma^2 c$ since not all the source is seen as the radiation for a relativistically moving object is beamed. Second, the photons in the local frame are softer by a factor of γ, and therefore only a small fraction of them, at the high energy tail, have enough energy to create pairs. The combination of these two effects reduces the optical depth by a factor of $\sim \gamma^{6.5}$. Therefore, the optical depth is reduced below unity, and the "compactness problem" is solved, if the Lorentz factor is larger than about a hundred.

This solution led to a three stage generic scenario for GRBs. First, a compact source releases about 10^{52} erg, in a small volume of space and on a short time scale. This large concentration of energy expands due to its own pressure. If the rest mass that contaminates the site is not too large, $\leq 10^{-5} M_{\odot}$, this will result in relativistic expansion with $\gamma > 100$. Finally, at a large enough radius, the kinetic energy of the expanding material is converted to internal energy an radiated, mainly in γ-rays. At this stage the system is optically thin and high energy photons can escape.

In this talk we will concentrate mainly on the third stage. We will assume that a relativistic flow with a high Lorentz factor exists, carrying more than 10^{52} erg as kinetic energy, and discuss how this flow may produce the γ-ray photons as well as the afterglow. This presentation will be short in equations, stressing the main qualitative ideas.

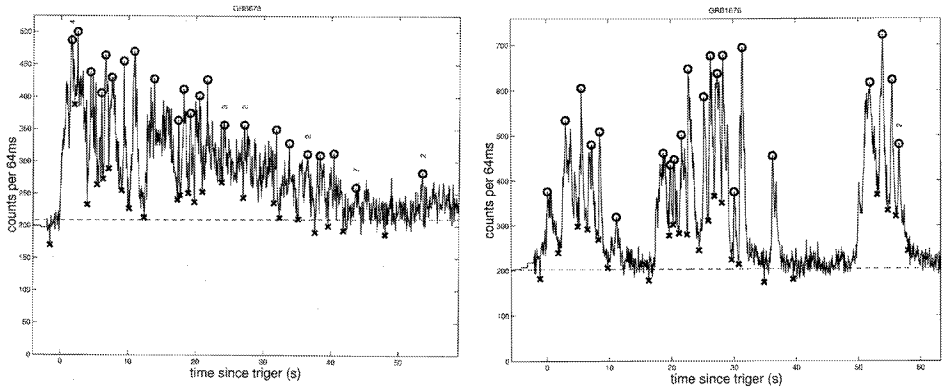

FIGURE 1. Two variable bursts, measured by BATSE. The dashed line is the background level.

II INTERNAL VS. EXTERNAL SHOCKS

Assume a flow carrying 10^{52} erg as kinetic energy. In order for this to produce photons, the kinetic energy must be converted back into internal energy and radiated away. The flow must therefore, at least partially, slow down. Two scenarios were proposed for this deceleration: external shocks [5] and internal shocks [6,7]. In the external shocks scenario, the relativistic material is running into some (external) ambient medium, probably the interstellar medium or a wind that was emitted earlier by the progenitor. In the internal shocks scenario the inner engine is assumed to emit an irregular flow, that consists of many shells, that travel with a variety of Lorentz factors and therefore colliding into each other and thermalizing some of their kinetic energy.

The property that proved to be very useful in constraining these two possibilities is the variability observed in many of the bursts. In the external shocks scenario, this variability is attributed to irregularities in the surrounding medium, e.g., clouds. Each time the ejecta runs into a higher density environment, it produces a peak. In the internal shocks scenario, the source has to emit many shells, and when every two of them collide, a peak is produced. External shocks require a complicated surrounding with a relatively simple source that explodes once, while internal shocks require a more complicated source that will explode many times to produce several shells. Due to these very different requirements from the source, the question of internal or external shocks is of fundamental importance in understanding the basic nature of the phenomena.

The size of the clouds in which the ejecta runs into, in the external shocks scenario, has to be very small to produce peaks that are narrower than the duration of the burst [8]. Sari & Piran [9] gave the following argument: The size of the clouds has to be smaller than $R/N\gamma$ to produce peaks that are narrower by a factor of N than the duration of the burst. The number of clouds should be smaller than N otherwise pulses arriving from different clouds will overlap and the amplitude of the variability will be reduced. Finally the observable area of the ejecta, due to relativistic beaming is $(R/\gamma)^2$. The maximal efficiency of the external shocks scenario is therefore given by (cloud area) $\times$(number of clouds)/(shell area)$\leq$ $1/N \sim 1\%$. Since in many bursts $N > 100$, external shocks have a sever efficiency problem, when constructed to produce highly variable bursts. Other predictions of external shock are also inconsistent with the observed temporal profile [10]. Moreover, the density ratio between the cloud and the surrounding has to be huge, of the order of $\gamma N^2 \sim 10^6$, in order that the ejecta will be slowed down mainly by the dense clouds rather than by the low density uniform medium.

Internal shocks do not suffer from these problems. The variability can be produced even without breaking the spherical symmetry. Detailed calculations show that the observed temporal structure coming from internal shocks, closely follows the operation of the inner engine that generated the shells [11]. In this scenario, the source must be variable on time scales shorter than a second and last for as long as 100 seconds, just as the bursts themselves.

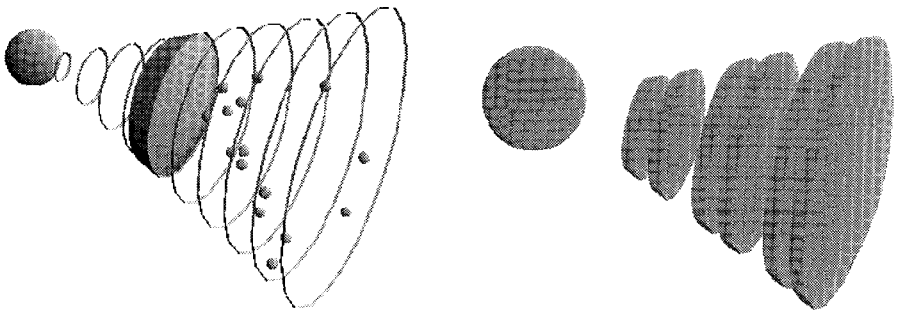

FIGURE 2. Producing variability by external shocks (left) or internal shocks (right).

III THE AFTERGLOW REVOLUTION

The study of γ-ray bursts was revolutionized when the Italian Dutch satellite BeppoSAX delivered arcminutes positioning of some GRBs, within a few hours time scale. This enabled other ground and space instruments to monitor the relatively narrow error box. Emission in X-ray, infrared, optical and radio, so called "afterglow" was observed by now for about a dozen of bursts. The study of GRBs, that was up to then collimated to a narrow energy band, immediately turned into a multi wavelength astronomy field. Due to the transient nature of the afterglow, a major part of the game is to observe the GRBs field early enough, when the afterglow is still bright. Within the first day, the optical emission is usually brighter than 20th magnitude and therefore small telescopes can play an important role in measuring the lightcurve. A large worldwide collaboration is observing these events and the data is submitted to an impressive Global-Coordinate-Network [12] in real time, allowing other observatories to react accordingly.

The observed afterglow usually shows a power law decay $t^{-\alpha}$ in the optical and X-ray where a typical value is $\alpha \cong 1.2$. Some afterglows show a steeper decline with $\alpha \cong -2$. On the radio wavelength, the flux seems to rise on timescale of weeks and then decay with a similar powerlaw. In some cases the radio flux was observed for about a year following the few seconds GRB.

The Afterglow was predicted well before it was observed [13–16] After the internal shocks produced the GRB, the shell interacts with the surrounding medium and decelerates. The emission shifts into lower and lower frequencies. Excitingly, the afterglow theory is relatively simple. It deals with the emission on timescale much longer than those of the GRBs. The details of the complex initial conditions are therefore forgotten and the description depends on a small number of parameters, such as the total energy and the external density.

The basic model assumes that electrons are accelerated by the shock into a powerlaw distribution $N(\gamma_e) \sim \gamma_e^{-p}$ for $\gamma_e > \gamma_m$. The lower cutoff of this distribution is assumed to be a fixed fraction of equipartition. It is also assumed that a con-

siderable magnetic field is being built behind the shock, it is again characterized by a certain fraction ϵ_B of equipartition. The relativistic electrons then emit synchrotron radiation which is the observed afterglow. The broad band spectrum of such emission was given by Sari, Piran & Narayan [17].

At each instant, there are three characteristic frequencies: (I) ν_m which is the synchrotron frequency of the minimal energy electron, having a Lorentz factor γ_m. (II) The cooling time of an electron is inverse proportional to its Lorentz factor γ_e. Therefore, electrons with a Lorentz factor higher than a critical Lorentz factor $\gamma_e > \gamma_c$ can cool on the dynamical timescale of the system. This characteristic Lorentz factor corresponds to the "cooling frequency" ν_c. (III) below some critical frequency ν_a the flux is self absorbed and is given by the Rayleigh-Jeans portion of a black body spectrum. The broad band spectrum of the well studied GRB 970508 [18] is in very good agreement with the theoretical picture.

The evolution of this spectrum as a function of time depends on the hydrodynamics. The simplest, which also well describes the data, is the adiabatic model with a constant density surrounding medium. The rest mass collected by the shock at radius R is about $R^3\rho$. On the average, the particles move with a Lorentz factor of γ^2 in the observer frame and therefore the total energy is given by $E \sim \gamma^2 R^3 \rho c^2$. Assuming that the radiated energy is negligible compared to the flow energy, we

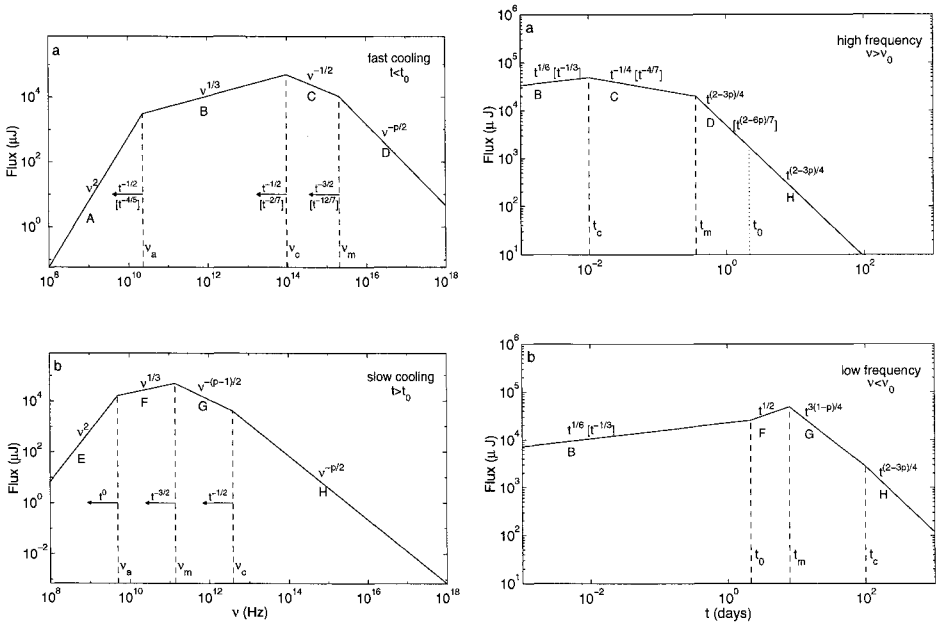

FIGURE 3. Theoretical spectra (left) and light curves (right) of synchrotron emission from a powerlaw distribution of electrons. $p = 2.2 - 2.4$ fits well the observed spectra and lightcurves.

obtain that $\gamma \sim R^{-3/2}$ or in terms of the observer time, $t = R/\gamma^2 c$, we get $\gamma \sim t^{-3/8}$. If on the other hand the density drops as R^{-2} (as is expected if the surrounding is a wind produced earlier by the progenitor of the burst) we get $\gamma \sim t^{-1/4}$. These simple scaling laws lead to the spectrum evolution as given in the above figure.

Given the above hydrodynamic evolution, one can construct light curves at any given frequency. These will also consist of power laws, changing from one power law to the other once the break frequencies sweep through the observed band. These power laws are in fair agreement with afterglow observations.

IV JETS AND BEAMING

The hydrodynamic evolution described above, assumed spherical symmetry. Scenarios in which the ejecta is not spherical but has a limited solid angle $\Omega = \pi\theta_0^2$ are usually called "jets". These "jets", should not be confused with the relativistic beaming of the radiation. The term "jet" corresponds to the physical shape of the outflow, and is created by the inner engine. In contrast, the relativistic beaming is a special relativity effect and has to do only with the fact that the ejecta is moving with relativistic Lorentz factor γ. The relativistic beaming allows an observer to see only a small angular extent, of size $1/\gamma$ centered around the line of sight.

The question of "jets" has two important implications. First, the true total energy emitted by the source is smaller by a factor of $\Omega/4\pi \sim \theta_0^2/4$ than if the ejecta was spherical. Second, the event rate must be bigger by the same factor to account for the observed rate.

Interestingly, due to the relativistic beaming (which is independent of jets) we are only able to see an angular extent of $1/\gamma < 0.01$ during the GRB itself where

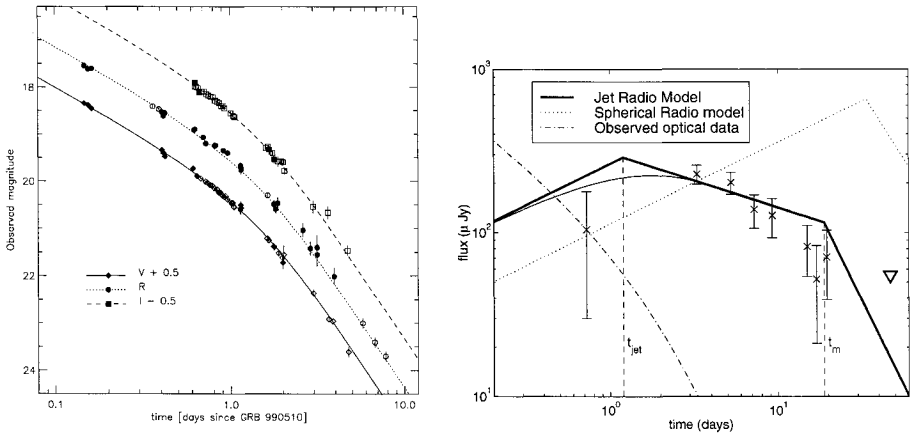

FIGURE 4. GRB 990510, the best evidence for a "jet": an achromatic break in optical and radio at $t_{jet} \cong 1.2$days implying $\theta_0 \cong 0.08$.

the Lorentz factor $\gamma > 100$. Therefore, we cannot distinguish a jet from spherical ejecta. Therefore, given the bursts only, the event rate and the energy in each GRBs are unknown to about four orders of magnitude! However, as γ decreases it will eventually fall below the inverse opening angle of the jet. The observer will appreciate that some of the sphere is missing from the fact that less radiation is observed. This effect, will produce a significant break, steepening the lightcurve decay by a factor of $\gamma^2 \sim t^{-3/4}$. The transition should occur when $1/\gamma = \theta_0$ and it therefore provides an indication for the jet's opening angle. Additionally, Rhoads [19] has shown that at about the same time, the physical size of the jet will begin to increase so that $\theta(\hat{t}) \sim 1/\gamma$. Taking this effect into account, the break is even more significant and the decay is proportional to $t^{-p} \sim t^{-2.2} - t^{-2.4}$.

Evidence of a break from a shallow to a steep power law was seen in GRB 990123 [4,20], unfortunately the break was observed only in one optical band while data on other bands were ambiguous. A very clear break was seen in GRB 990510 [21,22] simultaneously in all optical bands and in radio. In GRB 990123 and GRB 990510 the transition times were about 2.1days and 1.2days reducing the isotropic energy estimate by a factor of ~ 200 and ~ 300 respectively.

Sari, Piran, & Halpern [23] have noted that the observed decays in GRBs afterglow that do not show a break are either of a shallow slope of $\sim t^{-1.2}$ or a very steep slope of $\sim t^{-2}$. They argued that the rapidly decaying bursts are those in which the ejecta was a narrow jet and the break in the light curve was before the first observations. Interestingly, evidence for jets are found when the inferred energy (without taking jets into account) is the largest. This implies that the jets account for a considerable fraction of the wide luminosity distribution seen in GRBs, and the true energy distribution is less wide than it seems to be.

V THE OPTICAL FLASH & THE RADIO FLARE

An exiting event this year was the first detection of a bright (9th magnitude) optical emission simultaneous with GRB 990123 [24]. Theoretical prediction for such a flash was recently given in detail by Sari & Piran [25,26] and was earlier suggested as a possibility by Mészáros & Rees [16]. During the first few tens of seconds, the evolution of the Lorentz factor as a function of time is not self similar. There are two shocks: a forward shock going into the surrounding medium and a reverse shock going into the expanding shell. The hydrodynamic details were discussed in [27]. During the initial stage, the internal energy stored behind the shocked surrounding matter and the shocked ejecta is comparable. However, the temperature of the shocked ejecta is much lower, typically by a factor of $\gamma \sim 10^2$. This results in an additional emission component with a typical frequency lower by a factor of $\gamma^2 \sim 10^4$, which, for typical parameters, falls in the optical regime. Contrary to the "standard" late afterglow, this emission is very sensitive to the initial Lorentz factor.

The optical flash of GRB 990123 peaked around 60 seconds after the burst trigger.

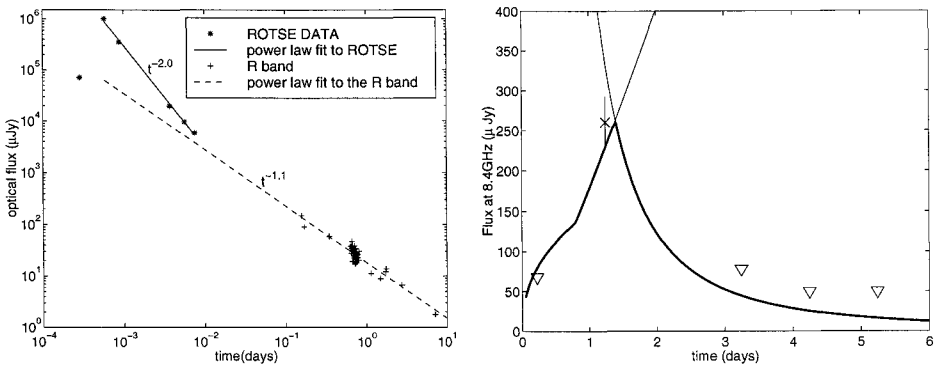

FIGURE 5. GRB990123: Optical (left) date fits theoretical prediction. Radio "flare" seen a day after the burst agrees with theory scaling of optical data (heavy solid line).

The observed optical properties of this event are well described by the emission from the reverse shock that initially decelerates the ejecta, provided the initial Lorentz factor is about 200 [28,29]. It takes tens of seconds for the reverse shock to sweep through the ejecta and produce the bright flash. Later, the shocked hot matter expands adiabatically and the emission quickly shifts to lower frequencies and considerably weakens.

Another new ingredient that was found in GRB 990123 is a radio flare [30]. Contrary to all other afterglows, where the radio peaks around few weeks and then decays slowly, this burst had a fast rising flare, peaking around a day and decaying quickly. Within a day the emission from the adiabatically cooling ejecta, that produced the 60s optical flash shifts into the radio frequencies [28]. The optical flash and the radio flare are therefore related. The fact that the "usual" forward shock radio emission did not show up later, on a timescale of weeks, is in agreement with the interpretation of this burst as a "jet" which causes the emission to considerably weaken by the time the frequency arrives to the radio.

VI POLARIZATION - A PROMISING TOOL

An exciting possibility to further constrain the models and obtain a direct proof to the geometrical picture of "jets" is to measure polarization. Gruzinov & Waxman and Medvedev & Loeb [31,32] considered the emission from spherical ejecta which by symmetry should produce no polarization on the average. Polarization is more natural if the ejecta is a "jet" and the observer is not directed at its very center [33–35] since the spherical symmetry is broken. For simplicity, lets assume that the direction of the magnetic field behind the shock is larger in the shock plane (the results are more general, unless the magnetic field has no preferred direction). The synchrotron polarization from each part of the fireball, which is perpendicular to

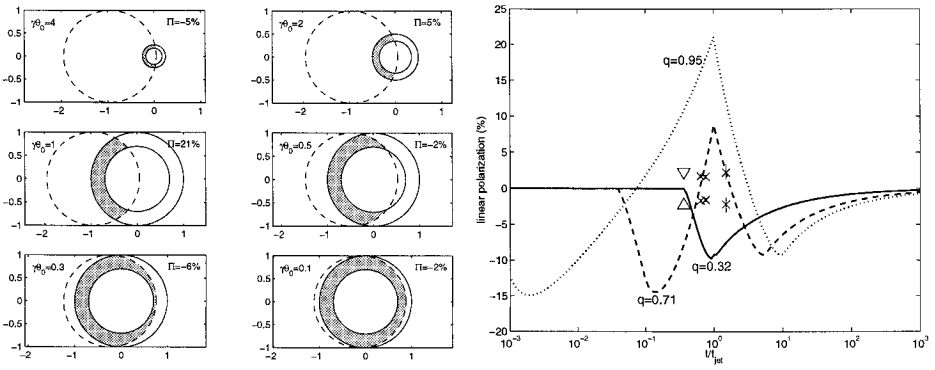

FIGURE 6. Left: Evolution of the observed ring (gray) and the physical jet (dash). Right: observed and theoretical polarization lightcurve.

the magnetic field, is directed radially.

As long as the relativistic beaming of size $1/\gamma$ is narrower than the physical size of the jet θ_0, one is able to see a full ring and therefore the radial polarization averages to zero. As the flow decelerates, the relativistic beaming $1/\gamma$ becomes comparable to θ_0 and only a part of the ring is visible. Net polarization is then observed. Note that due to the radial direction of the polarization from each fluid element, the total polarization is maximal when a quarter or three quarters of the ring are missing (or radiate less efficiently) and vanishes for a full or half ring. The observed polarization when more than half of the ring is missing is perpendicular to the direction when less than half of it is missing.

At late stages the jet expands and since the offset of the observer from the physical center of the jet is constant, spherical symmetry is regained. The vanishing and re-occurrence of significant parts of the ring results in a unique prediction: there should be three peaks of polarization, with the polarization position angle during the middle peak rotated by 90° with respect to the other two peaks. In case that the observer is very close to the center, more than half of the ring is always observed, and therefore only a single direction of polarization is expected. Few possible polarization light curve are presented in the figure.

VII WHAT DID WE LEARN ABOUT THE SOURCE?

(i) Internal shocks imply that the source is variable on < 1s timescales but lasts for tens of seconds. (ii) The event rate is probably higher than observed by about a factor of a hundred since some events are narrow jets. This translates to one event per 10^5 years per galaxy (iii) The environment of at least some bursts well agrees with ordinary ISM densities. These bursts do not occur in their galaxies' halo. (iv) measurements of optical flashes and radio flares probe the ejecta material, allowing

us to measure how many baryons reside in the explosion cite. GRB 990123 has $\gamma_0 \sim 200$. (v) Taking jets into account, the total energy involved can be "only" 10^{52}erg even in the most extreme case.

REFERENCES

1. Klebesadel, R. W.; Strong, I. B. & Olson, Roy A. 1973, ApJ, 182, 85
2. Paciesas, W. S. et al. 1999, ApJS, 122, 465
3. Band, D. et al., 1993, ApJ, 413, 281
4. Kulkarni, S. R., et al. 1999, Nature 398, 389
5. Mészáros, P., & Rees, M. J. 1993, ApJ, 405, 278
6. Narayan, R., Paczyński, B. & Piran, T. 1992, ApJ, 395, 83
7. Rees M. J. & Mészáros P. 1994, ApJ, 430, L93
8. Fenimore, E. E., Madras, C., & Nayakshine, S. 1996, ApJ, 473, 998
9. Sari, R., & Piran T. 1997, ApJ, 485, 270
10. Ramirez-Ruiz, E., & Fenimore, E. E. 1999, A&A, 138, 521
11. Kobayashi, S., Piran, T., & Sari, R. 1997, ApJ, 490, 92
12. Barthelmy, S.D., et al. 1994, in "Proceeding of the Second Huntsville Workshop"; eds. G.Fishman, J.Brainerd, K.Hurley; 307; 643
13. Paczyński, B. & Rhoads, J. 1993, ApJ, 418, L5
14. Katz, J. I., 1994, ApJ, 422, 248
15. Vietri, M. 1997, ApJ, 478, L9
16. Mészáros, P., & Rees M. J. 1997, ApJ, 476, 232
17. Sari, R., Piran, T. & Narayan, R. 1998, 497, L17
18. Galama, T. J. et al. 1998, ApJ, 500, 101
19. Rhoads, J. E. 1999, ApJ, 525, 737
20. Fruchter, A. S., et al., 1999, ApJ, 519, L13
21. Stanek, K. Z., Garnavich, P. M., Kaluzny, J., Pych, W. & Thompson, I. 1999, ApJ, 522, L39
22. Harrison F. A., et al. 1999, ApJ, 1999, 523, L121
23. Sari, R., Piran, T., & Halpern, J. 1999, ApJ, 1999, 519, L17
24. Akerlof, C. et al., 1999, Nature. 398, 400
25. Sari, R., & Piran T. 1999a, A&AS, 138, 537
26. Sari, R., & Piran T. 1999b, ApJ, 520, 641
27. Sari, R., & Piran T. 1995, ApJ, 455, L143
28. Sari, R., & Piran T. 1999c, ApJ, 517, L109
29. Mészáros, P., & Rees M. J. 1999, MNRAS, 306, L39
30. Kulkarni, S. R., et al. 1999, ApJ, 522, L97
31. Gruzinov A., & Waxman E., 1999, ApJ, 511, 852
32. Medvedev, M. V., & Loeb A., 1999, astro-ph/9904363
33. Gruzinov A. 1999, ApJ, 525, L29
34. Ghisellini, G., & Lazzati, D., 1999, MNRAS, 309, L7
35. Sari, R. 1999, ApJ, 524, L43